Integrated absorption-energy transport measurements from ultra-intense laser heating of atomic clusters

A S Moore, E L Clark, R D Edwards, R T Eagleton, E T Gumbrell

AWE plc, Aldermaston, Reading, RG7 4PR, UK

P M Nilson, J Lazarus, R A Smith

Blackett Laboratory, Imperial College, London SW7 2BZ, UK

R J Clarke

Central Laser Facility, CCLRC Rutherford Appleton Laboratory, Chilton, Didcot, Oxon., OX11 0QX, UK

Main contact email address: *alastair.moore@awe.co.uk*

Introduction

Atomic clusters are well known for their ability to absorb a very high fraction of the laser energy incident upon them (>90%)[1]. Consequently, a radically different laser interaction occurs in comparison to that found when gas targets or solid targets are used. Gases, which typically absorb <1% of the incident laser energy, produce relatively low temperature plasma, while solid density targets are heated far more efficiently through a variety of heating mechanisms.

A single atomic cluster presents a small sub-wavelength scale, solid density target. This significantly modifies the energy transport away from the case of a solid density foil interaction. A gas consisting of many thousands of atomic clusters can therefore be heated very efficiently to produce a low average density high temperature plasma. Substantial work studying high intensity laser interactions with atomic clusters has identified them as a bright and efficient x-ray source that can also produce MeV ion energies, enabling fusion experiments on a small scale[2].

Study of the laser absorption in a cluster medium was originally carried out in[1], where a sub-relativistic intensity (<10^{17} Wcm^{-2}) interaction was investigated. We report new investigations of energy absorption and transport that result from large, high Z cluster interaction extending previous work into the relativistic, ultraintense regime (>10^{18} Wcm^{-2}).

Experimental Details

The experiment was performed using the Vulcan Nd:glass Petawatt laser[3]. During the campaign this delivered up to 410 J in a 430 fs pulse. We utilized this to study two intensity regimes >10^{19} Wcm^{-2} (40 J) and >10^{20} Wcm^{-2} (400 J). In these two relativistic regimes the normalized vector potential a_0 is 10 and 40 respectively. The f/3.1 parabola was used to focus the beam to a 10 μm focal spot that contained more than 50% of the pulse energy. In the target chamber, a small part of the main beam was split and frequency-doubled to provide a sub-picosecond optical probe. This was split further into S and P polarizations, to enable two time-separated interferometric images to be taken on a single shot. With this arrangement we were also able to image the 90 degree side-scattered laser light from the plasma. Measurements of the laser energy were made inside the chamber using a large area pyroelectric joulemeter directly behind the gas jet target. When this was not fielded it was possible to obtain electron spectra from the interaction with an on-axis magnetic spectrometer. This was used in conjunction with a high resolution image plate detector (Fuji BAS1800II). A Thompson parabola was located at 90 degrees to the target normal, just above the injection of the probe, however no ions were detected throughout the experiment. The Thompson parabola was configured to only detect ion energies in excess of 100keV/nucleon. For the experiments we present in xenon, this corresponds to ion energies of more than 13 MeV, indicating that we were not able to sufficiently accelerate ions to this degree in the interaction.

In the experiment we examined the interaction of the laser pulse with a gas jet composed of xenon clusters. The gas jet was positioned 3mm below the focal spot of the laser, and the focus aligned to the centre of the gas jet spray. The gas jet was operated at room temperature and a backing pressure of 27 bar, producing a 45° plume of xenon clusters with an average radius of ~23 nm.

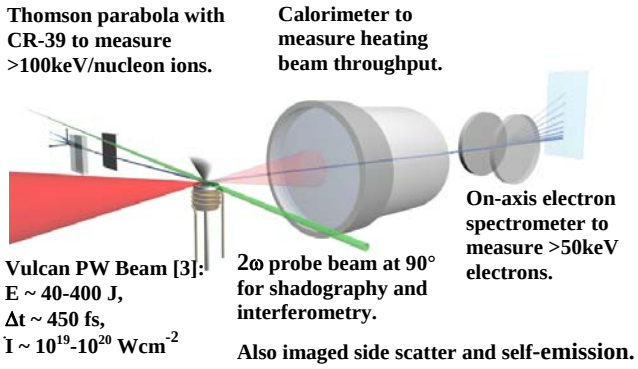

Figure 1. Illustration of the diagnostics fielded in the Petawatt target chamber for the experiment.

Energy Deposition in the Cluster Medium

When the gas jet was not fired, measurements of the laser energy using the joulemeter collected all the energy transmitted into the target chamber, and showed that > 400J was focused onto target. Repeat measurements with laser incident on the cluster jet measured less than 5 J of energy transmitted through the medium on high energy (> 400 J) shots. In addition, diagnostics in the laser system, showed that no considerable light was directly backscattered by the exploding cluster plasma. Side scatter/emission images, which are shown in Figure 3, also show evidence of low levels of scattered light. The collection efficiency of the side scatter imaging system, was approximately 2%, which implies that at most a few mJ were scattered into 4π. Therefore, building on the results of Reference [1], at this higher, ultra-relativistic intensity we still observe more than 90% absorption of the laser energy by the cluster medium. It is pertinent to note when comparing these results that the laser pulse duration was ~ 2 ps in Reference [1].

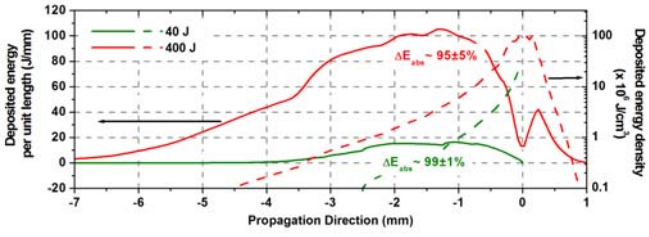

Figure 2. Calculated energy deposition through the focus using the focal-integration shell and incorporating the Nanoplasma model.

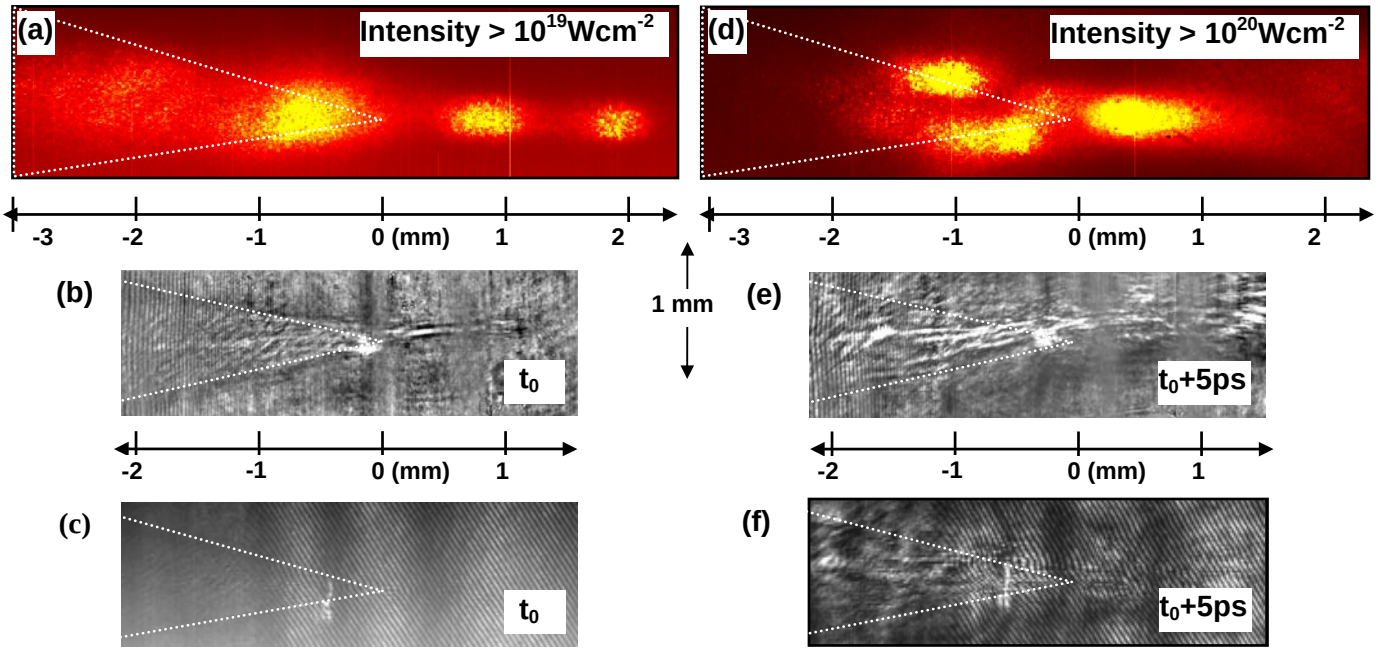

Figure 3. Images of 90° side-scatter filtered at 1053±10nm (a, d), 2ω probe images: shadowgram (b, d) and interferometric (c, f) of the laser-cluster interaction at 40 J (a,b,c) and 400 J (d,e,f) show fast energy transport and significant structure to the interaction.

In comparison the Vulcan Petawatt has a pulse duration (FWHM) of ~ 450 fs, which will have a significant impact on the individual cluster explosion and is the likely explanation for the difference between these results[4].

Previous work has used the analytical nature of a Sedov-Taylor blast wave to measure the energy deposition per unit length[5]. However, due to the very high absorption and fast transport, the timescales that we were able to observe, were much shorter than that required for a blast wave formation precluding us from estimating the energy deposition in this way. Consequently, we model the absorption using a focal-integration model and employing the well-established nanoplasma model[6], with an added relativistic mass correction, to evaluate the amount of energy absorbed by each cluster.

The microscopic size of clusters results in a much greater absorption cross-section than that for scattering[7]. Consequently although the model does not include any defocusing effects, any defocused light that is refracted outside the focal volume, will also be strongly absorbed. The pre-pulse, which we were able to characterise using the cluster medium in these experiments[8], will likely exacerbate this effect by producing a cool plasma on the laser-axis at best focus prior to the main interaction.

The nanoplasma model has to be used with a degree of caution since hydrodynamic forces must dominate in the cluster explosion in order for it to be valid. Energy deposition into free electrons is calculated through treating the cluster as a dielectric sphere within a constant electric field. This is appropriate provided the cluster is much smaller than the laser wavelength and (anomalous) skin depth, but larger than the Debye length. Traditionally this is therefore most appropriate for large clusters. However, at the ultra-high intensities we study here, both the plasma temperature and the ponderomotive force of the laser are detrimental to this propriety. By comparison of the ponderomotive potential with that of the charged cluster sphere, we calculate that for the lower energy 40 J experiments, as the pulse propagates through the cluster medium, the fraction of electrons that free-stream out of the clusters is at most 25% . By this point in the interaction, the clusters will have expanded sufficiently that hydrodynamic forces will dominate and the nanoplasma model can be used. For the more energetic experiments, it is less certain that the nanoplasma model is appropriate, since significant ionisation occurs very rapidly, leading to coulomb forces being a greater contribution to the explosion.

Using the modified nanoplasma model the energy absorbed per cluster as a function of intensity is calculated. The focal-integration shell estimates the number of clusters that experience a certain intensity through the focal region of the laser pulse. By incorporating this with the nanoplasma model results, the total energy absorbed by the medium can be directly estimated. For consistency this model was tested and found to be in good agreement with the energy deposition studies in Reference [5].

Results of the focal-integration model in both of the regimes studied are shown in Figure 2. The most notable result is that owing to the very high intensity for a number of Rayleigh lengths either side of the focus, there is substantial energy deposition many millimeters away from focus (z = 0). Owing to the tight focusing geometry of the Vulcan Petawatt, a macroscopic plasma forms with a volume ~ 12 mm^3. For both the 40 J and 400 J shots Figure 2 shows how the energy deposited per unit length is depleted prior to reaching the focus. However, due to the smaller volume of the interaction at the focus the highest energy density still occurs here. For the 400 J case, Figure 2 shows energy is in fact deposited both sides of the focus, since energy still remains beyond z = 0. Evidence for this is also apparent in Figure 3(d) where substantial light is scattered just beyond the focus at z = 0.5mm.

Energy Transport

The transport of energy away from the interaction region was measured through self-scatter and optical probing. Shadowgraph and interferometric images in Figure 3 obtained using the frequency-doubled probe light are in good agreement with the focal-integration modelling and show the large extent of the interaction. Figure 3(a) and (b) show 1053nm side-scattered light for the 40 and 400 J cases and emphasise the radically different nature of the interaction at these two intensities.

The combination of the low intensity threshold for absorption in clusters[1], and the pre-pulse level measured on the PW, is sufficient that when full energy shots were fired, a significant plasma was observed up to 700 ps prior to the arrival of the peak intensity[8]. This has quite a dramatic effect on the

interaction. As illustrated by the side-scatter images in Figure 3(d), the structure of the interaction shows evidence of the pre-pulse destroying clusters on-axis, at the focus so little light is scattered. However, in the lower intensity wings of the pulse at z = -1 mm, significant emission implies a more substantial interaction, resulting from the main pulse interacting directly with clusters. The shadowgraph image in Figure 3(e) shows the large-scale, multi-filament plasma that results after the arrival of the main pulse.

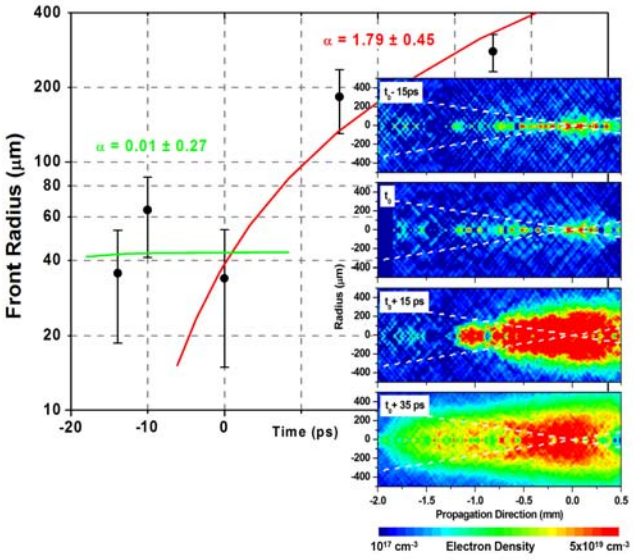

Figure 4. Trajectory of the fast ionisation wave propagating at ~ 10^7 ms^{-1} produced by the interaction at 10^{19} Wcm^{-2} and four spatial profiles of the electron density at time t_0-15ps, t_0, t_0+15ps and t_0+35ps, showing that prior to the main pulse interaction at t_0, there is no significant interaction.

By reducing the energy from 400 J to 40 J, it was found that the pre-pulse could be reduced sufficiently to change the interaction. This is can be seen in the change in the structure in Figure 3(a) and (d). The critical power for relativistic self-focusing is still surpassed many times even in this lower intensity regime and the side emission in Figure 3(a) shows strong evidence of self focusing. The fast focusing of the laser results in a Rayleigh length of l_R~ 0.02 mm. The three-bead structure in the side-scatter image shows clearly that energy is transported over ~ 1 mm ($50l_R$) between the three emitting centres. In addition to ω scattered light, the image may include contributions from bright Raman side-bands, shifted by Δλ~5-50nm, and which are not adequately suppressed by the 1053nm filter. In Reference [9] such Raman shifted side-scatter was shown to be a strong signature of self-focusing, being generated most strongly at the end of the self-focused channel.

Interferograms like that shown in Figure 3(c), of the lower intensity interaction, were obtained at several different times, enabling the plasma expansion to be studied. These are deconvolved to show the spatial profile of the electron density in Figure 4. Figure 4 also shows the trajectory obtained with a power law ($r \sim t^{\alpha}$) fit to the evolution of the ionisation front radius either side of the interaction. The expansion velocity measured from this approaches 10^7 ms^{-1}, and the power law fit shows that on the timescale we were able to study, the front appears to be accelerating ($\alpha>1$). In Reference [10] a similar fast ionization front was observed from argon clusters irradiated at 10^{16} Wcm^{-2}. This was a result of free streaming electrons. The high temperature within each cluster generates electrons with a mean free path that is greater than the temperature scale-length of the plasma enabling them to travel uninhibited through the heated plasma, and ionise the surrounding plasma. This produced a characteristic preheat ahead of the ionisation front, though we do not observe such a non-local precursor in the data we present. It is uncertain whether the expansion we measure is due to the radial component of the ponderomotive force driving electrons out of the focus, a large radiation flux, resulting from the high Z of xenon, ionizing the surrounding medium, or rapid, diffusion-like electron transport resulting from the high energy deposition. Indeed, the fact that the front appears to accelerate may be due to the transition between these regimes.

For both intensity cases we investigate, $a_0 > 1$, and so the **v** x **B** terms in the Lorentz force cannot be ignored. These contribute a longitudinal component to the ponderomotive potential, in addition to the radial component, which accelerates electrons in the propagation direction. In a short-pulse laser interaction, electrons can rapidly escape from the interaction region gaining U_p [11].

$$U_p = (\sqrt{(1+a_0^2)}-1)m_e c^2 = e^2 E_0^2/(4\gamma m_e \omega^2) \qquad (1)$$

For the two cases we investigate $U_p \sim 3$ and 30 MeV.

The on-axis electron spectrometer allowed measurements of the electron spectrum in the range between 0.1 and 100 MeV. A number of spectra were obtained on 400 J shots, a typical example of which is shown in Figure 5. The most notable feature is the broad peak centred at ~ 0.5 MeV. Below 0.4 MeV a non-relativistic Maxwellian function - $f(E) \sim E^{1/2}\exp(-E/kT_{NR})$ can be fitted to estimate a temperature of T_{NR} ~ 30 keV. However, the higher energy data cannot be so easily interpretted using a relativistic Maxwellian - $f(E) \sim E^2 \exp(-E/kT_R)$ as illustrated by the green and red curves in Figure 5.

Solid target interactions in the ultra-relativistic regime produce ponderomotively driven electron acceleration that can generate a Maxwellian distribution on-axis with a temperature equal to U_p. Gas target interactions at similar intensities can be tuned to produce monoenergetic electron beams accelerated by a relativistic plasma wave to energies between 50 and 80 MeV [12].

Neither such description seems to be the case observed here. The spectrum we measure contains considerable structure at a much lower energy than other targets suggesting more collisions have distributed the energy to a greater number of particles. Two component structure in the electron spectrum from cluster explosions at much lower intensity (~10^{16} Wcm^{-2}), has previously been observed and explained using the nanoplasma model in which the electric field is enhanced inside the cluster when the density reaches $3n_{crit}$ [13]. However, not only did the resulting electron spectrum have a much sharper spike at high energy than that in Figure 5, it is likely that in the ultra-relativistic interaction from which we measure the electron spectra the clusters are fully stripped of electrons by the ponderomotive force and subsequently coulomb explode, resulting in the nanoplasma model being an invalid description.

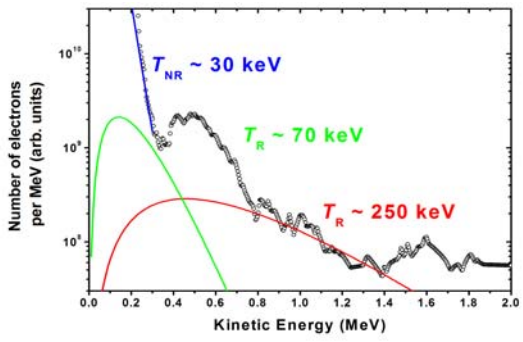

Figure 5. Electron spectrum at 0° from the laser axis from a 400 J PW laser-interaction with xenon clusters. A cool, non-relativistic distribution is shown in blue, and two higher energy relativistic distribution functions are shown in green and red.

The ion detection system had a relatively low sensitivity threshold and was insensitive to ions with energy less than 13 MeV. No high energy ions were measured from the interaction.

The sub-relativistic distribution of electrons and apparent absence of very fast ions implies that a significant proportion of the laser energy remains in the plasma and does not produce high energy particles. Initially laser energy is unable to escape due to the large absorption cross-section of clusters, so that after multiple scattering almost all the laser energy is absorbed. This in combination with the very early onset of absorption before the focus results in energy being distributed in a large volume. A very large number of electrons and subsequently ions are therefore heated but in the relatively low intensity interaction region mm's before the focus. In the case of the lower energy, 40 J investigations, energy deposition modelling showed that, relatively little laser energy remained once the pulse reached the focus. Consequently, in the region in which the majority of energy is deposited, the large xenon clusters explode hydrodynamically making it seem unlikely that electrons or ions would experience significant acceleration. Subsequent self-focusing observed in the self-emission images will prevent the laser field interacting with many clusters, producing very few high energy electrons.

The 400 J interactions are more complicated to interpret. Again the laser energy is almost all absorbed, now over an even larger volume than in the lower intensity results. The pre-pulse measured on full-energy laser shots adds to the difficulty in interpreting the data, since it is possible that many of the clusters will have been destroyed entirely before the arrival of the main pulse. It is likely that clusters in the wings of the gas jet undergo a quasi-hydrodynamic/coulomb explosion, while at the focus the xenon atoms will be completely stripped of electrons and any clusters that remain after the pre-pulse interaction will explode predominantly due to coulomb forces.

While the focal-integration shell and nanoplasma modelling have provided good agreement with the absorption data, we note that this stretches the applicability of the model since it is unable to account for certain physics. PIC modelling at lower intensities, but also in the regime between pure hydrodynamic and pure coulomb explosion mechanisms, has proposed collisionless heating methods by which clusters absorb energy[14]. In addition, while we correct the electron mass to take account of relativistic velocities, we are unable to include the magnetic field, and v x B forces that will inevitably effect the heating rate and electron acceleration mechanisms at these intensities.

Conclusions

In conclusion, we have made the first measurements of energy deposition in a high Z cluster medium using an ultra-relativistic laser pulse. The results, although contrary to previous predictions, are well matched by the focal integration shell used in conjunction with the nanoplasma model.

Images of the plasma density and side-scattered laser light show that the pre-pulse present on 400 J, PW shots has a significant effect on the interaction, but does not prevent the > 90% absorption. When the energy is reduced to 40 J images of side-scattered light show the interaction changes and shows characteristic signs of self-focusing of many Rayleigh lengths. Interferometric probe images at various times after the interaction show that a fast ionization front forms traveling at ~ 10^7 ms^{-1} and is still accelerating 35 ps after the interaction.

On-axis electron spectra show signs of structure with a peak at 0.5 MeV, which is not easily matched by an ultra- relativistic Maxwellian distribution function. A non-relativistic population also exists with a temperature of ~ 30 keV. Electron energies produced from conventional solid and gas target experiments are also unable to match those measured here.

Acknowledgements

The authors gratefully acknowledge the support of the operational staff at the Central Laser Facility. This work was funded by the UK MoD.

References

1. T. Ditmire *et al.*,
Phys. Rev. Letters 78 3121 (1997)

2. T. Ditmire *et al.*,
Nature. 386 54 (1997);
T. Ditmire *et al.*,
Nature. 398 489 (1999)

3. C. Danson *et al.*,
Nucl. Fusion 44 S239 (2004)

4. A.S. Moore *et al.*,
App. Phys. B 80 101 (2005)

5. J. Zweiback and T. Ditmire,
Phys. Plasmas 8 4545 (2001)

6. T. Ditmire *et al.*,
Phys. Rev. A 53 3379 (1996)

7. V.P. Krainov and M.B. Smirnov,
Phys. Reports 370 237 (2002)

8. J. Lazarus *et al.*,
CLF Annual Report 2004/2005, p 38

9. Z. Najmudin *et al.*,
CLF Annual Report 1999-2000, p 27

10. T. Ditmire *et al.*,
Phys. Rev. Letters 80 720 (1998)

11. G. Malka and J.L. Miquel,
Phys. Rev. Letters 77 75 (1996)

12. S. Mangles *et al.*,
Nature 431 535 (2004)

13. Y.L.Shao *et al.*,
Phys. Rev. Letters. 77 3343 (1997)

14. C. Jungreuthmayer *et al.*,
Phys. Rev Letters. 92 133401 (2004);
T. Taguchi *et al.*,
Phys. Rev. Letters. 92 205003 (2004)